ACS Photonics

Article

pubs.acs.org/journal/apchd5

Observation of Thermal Beaming from Tungsten and Molybdenum Bull's Eyes

Jong Hyuk Park,[†,‡,§] Sang Eon Han,[‡,∥] Prashant Nagpal,[‡,⊥] and David J. Norris*[,†]

[†]Optical Materials Engineering Laboratory, ETH Zurich, 8092 Zurich, Switzerland

[‡]Department of Chemical Engineering and Materials Science, University of Minnesota, Minneapolis, Minnesota 55455, United States

[§]Photo-Electronic Hybrids Research Center, Korea Institute of Science and Technology, Seoul, 136-791, South Korea

[∥]Department of Chemical and Biological Engineering, University of New Mexico, Albuquerque, New Mexico 87131, United States

[⊥]Department of Chemical and Biological Engineering, University of Colorado, Boulder, Colorado 80303, United States

Supporting Information

ABSTRACT: Although losses in plasmonic films can be detrimental for optoelectronics, they can be exploited to create novel thermal emitters. Surface plasmon polaritons that are thermally excited on a heated metal surface can be converted to photons with useful properties. We demonstrate highly tailored thermal emission from tungsten and molybdenum films patterned with a series of circular concentric grooves (i.e., a bull's eye). At 900 °C our structures emit an infrared beam normal to the film that is spectrally narrow (tens of nanometers) and highly directional (~2° angular divergence). The peak wavelength (3.5 μm) can be tuned with groove periodicity. To enhance the thermal stability of the structures, we add a thin layer of HfO_2. Such devices, with their simple design and low thermal mass, provide interesting incandescent light sources for various applications.

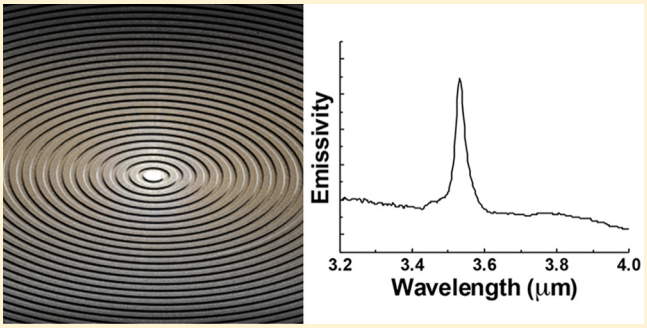

KEYWORDS: *optical beaming, bull's-eye pattern, plasmonics, thermal emission, surface plasmon polaritons, incandescent light sources*

Surface plasmon polaritons (SPPs) are hybrid electron−photon waves that exist on a metallic interface.[1] By patterning the metal, the propagation of SPPs can be controlled and manipulated.[2] In particular, SPPs can concentrate electromagnetic fields to volumes well below the diffraction limit of light.[3,4] Thus, patterned metallic films have been explored for nanophotonics.[5] This is motivated in part by the facile conversion of SPPs to photons and vice versa. However, significant energy can be lost in plasmonic devices due to ohmic resistance in the metal. While this is typically a disadvantage, it can sometimes be beneficial. For example, according to Kirchhoff's law, the emissivity of a structure is equal to its absorptivity.[6,7] Thus, if plasmonic losses enhance the optical absorption of a metallic film at specific wavelengths, this can be used to tailor its thermal-emission spectrum. This effect has been explored by heating specifically structured films.[8−11] SPPs that are thermally generated on the interface of such structures can then be converted to photons. (Surface phonon polaritons on polar surfaces have also been studied for this effect.[12,13]) The resulting modified thermal emission has potential use in thermophotovoltaic devices[9,14] or as novel incandescent light sources.[15−17] In the latter case, because plasmonic devices are typically thin with low thermal mass, SPPs can be thermally excited over the entire device or on a selected region with very little power.

To explore such devices, we previously considered[18] whether a common plasmonic structure, a bull's eye,[19−24] could provide a useful thermal emitter. We predicted that this structure, which consists of a series of equally spaced circular concentric grooves on a metallic surface, could lead to a highly directional monochromatic source of infrared light. According to our simulations, the grooves can act as a diffraction grating for thermally excited SPPs on the interface, causing photons to be emitted from the surface. Due to the circular symmetry, only the emission normal to the surface of the bull's eye should be strong. The peak wavelength in the normal direction should be close to the period of the grooves for first-order SPP diffraction. We referred to this effect as thermal beaming in analogy to optical beaming, which has been observed for visible light transmitted through a central aperture of a silver bull's eye.[19]

However, the predicted thermal beaming has not yet been confirmed by experiment. The simulations[18] treated idealized structures and neglected structural deterioration or oxidation that may occur in real materials at elevated temperatures.[25] Thus, it is unclear whether thermal beaming from bull's eyes is achievable in practice and, if so, how directional and narrowband the emission can be. Here, we address this by

Received: January 12, 2016
Published: February 17, 2016

DOI: 10.1021/acsphotonics.6b00022
ACS Photonics 2016, 3, 494−500

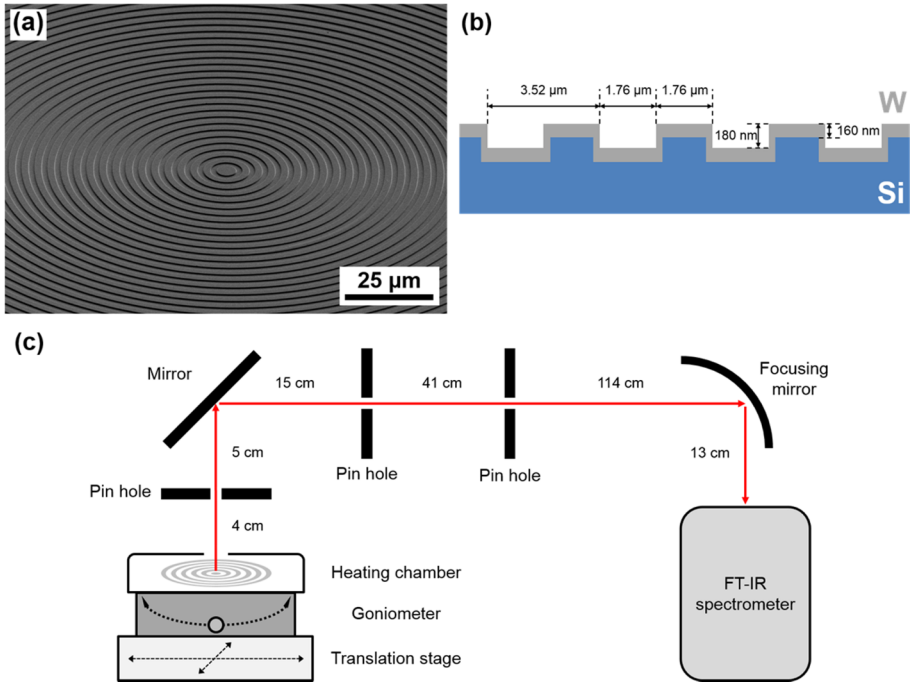

Figure 1. (a) Scanning electron micrograph of a W bull's eye, tilted 60° from normal. The entire structure has a diameter of ∼2.1 mm and contains 300 circular concentric grooves. (b) The structural parameters of the bull's eye: the period is 3.52 μm, the grooves are 1.76 μm wide by 180 nm deep, and the W layer is 160 nm thick. (c) Schematic of the experimental setup for measuring thermal-emission spectra. The diameter of each of the pin holes is ∼2.3 mm.

examining thermal emission from refractory bull's eyes. When heated to high temperatures, we indeed observe a highly directional and spectrally narrow beam of infrared light. The emission spectrum in the normal direction shows a single peak at a wavelength nearly identical to the period of the bull's eye, as predicted. The emission has a line width of tens of nanometers at 3.5 μm and decays rapidly as the emission angle is tilted from normal. Due to their directionality, such sources exhibit interesting optical coherence, as previously discussed.[12,18] Furthermore, we demonstrate the thermal stability of these structures during beaming by adding a protective oxide layer on the outer metallic surface. Therefore, we confirm that simple heating of a metallic bull's eye can provide a novel source of highly directional narrowband radiation. Such structures may be useful in various applications, such as molecular sensing and in situ temperature measurement.

RESULTS AND DISCUSSION

To realize thermal beaming, a material is needed that can withstand elevated temperatures, be patterned, and support SPPs at the target wavelength for the emission. The latter requires the real part of the dielectric function to be smaller than −1 at this wavelength.[26] To satisfy these conditions, tungsten (W) and molybdenum (Mo) are promising candidates. Both have high melting temperatures (3422 and 2623 °C, respectively), they support SPPs at wavelengths longer than ∼1 μm,[27] and they are inexpensive materials. Thus, with these metals, we followed our previous theoretical treatment[18] and designed structures targeting an emission wavelength of 3.5 μm. The exact geometry was optimized by numerical simulation to obtain a highly directional narrowband beam with large emissivity.

W and Mo bull's eyes were fabricated by the following procedure. Circular concentric grooves were patterned on silicon substrates via photolithography and reactive-ion etching (RIE). Then, a W or Mo layer was deposited on these patterned substrates by dc magnetron sputtering. The fill factor of the bull's eye, defined as the ratio of the width of the ridge to the period of the grooves, was adjusted to about 0.5 by tuning the process parameters of the photolithography. The depth of the grooves was controlled by varying the duration of the RIE. Detailed experimental conditions are provided in the Supporting Information.

Figure 1a shows a typical fabricated W bull's eye. It contains 300 circular concentric grooves with a period of 3.52 ± 0.01 μm; the diameter of the entire structure is ∼2.1 mm. The groove dimensions are described in Figure 1b. In general, the surface morphology of plasmonic structures plays a significant role in determining the loss of SPPs including the ohmic loss and unwanted scattering.[1,28,29] We characterized the surface of our films via atomic force microscopy (AFM). The flat areas next to the bull's-eye patterns were scanned; the surfaces in the patterned regions were assumed to be comparable. Figure S1 in the Supporting Information contains AFM images of the W and Mo films. Both films exhibited surfaces with a root-mean-square (RMS) roughness below 1.5 nm. We note that the bull's eyes could also have been prepared by direct patterning of metallic layers. However, since the etch rate in polycrystalline films is nonuniform, with this approach, the patterned grooves would be much rougher (RMS roughness of ∼10 nm), as we previously demonstrated.[30]

To measure the thermal-emission spectrum, the apparatus depicted in Figure 1c was used (see also Figure S2 in the Supporting Information). The sample was placed on a resistive heater in a heating chamber (Linkham Scientific, TS1500), which was mounted so that it could be tilted or translated. The emission was directed with mirrors through pinholes into a Fourier-transform infrared (FTIR) spectrometer (Bruker,

DOI: 10.1021/acsphotonics.6b00022
ACS Photonics 2016, 3, 494−500

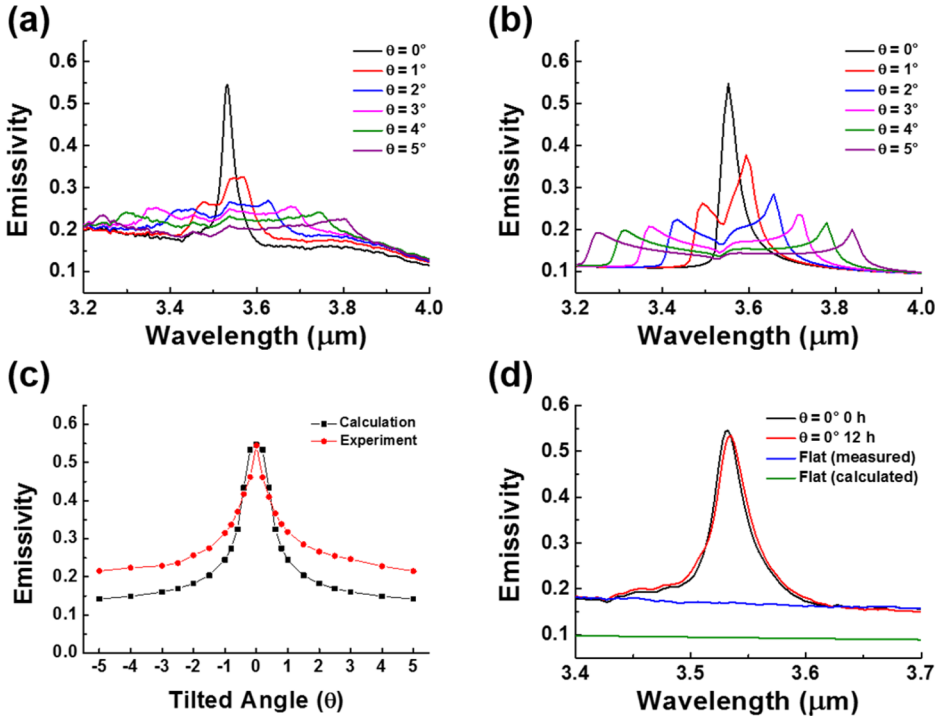

Figure 2. Thermal-emission spectra of a W bull's eye at 900 °C. The structural parameters were as in Figure 1b. (a) Measured thermal-emission spectra at various tilt angles (θ) from normal. The collection angle of the emission spectrum was ±0.1° and a carbon pellet was used to calibrate the emissivity. (b) Calculated thermal-emission spectra vs θ. The dielectric function of W at 900 °C was employed. (c) Angular dependence of the emissivity at the peak wavelength. (d) Comparison of the emission spectra initially and after 12 h at 900 °C. The measured and calculated emission spectra for a flat W film at 900 °C are also shown.

Vertex 80). Using the red laser beam coming from the interferometer in the spectrometer, the optics were aligned and the position and tilt angle of the sample adjusted. The atmosphere in the heating chamber was evacuated with a turbomolecular pump, and the sample was heated. The pinholes in the beam path were set to obtain a collection angle of ±0.1°.

Figure 2 shows the thermal-emission spectra of our W bull's eye at 900 °C. The emission spectra were measured at various tilt angles (θ) from normal (Figure 2a). To calibrate the emissivity, each emission spectrum was normalized by that of a reference emitter (pelletized carbon nanopowder), which was assumed to be a blackbody. The bull's eye exhibited a sharp emission peak in the normal direction. The peak was at 3.532 μm, nearly identical to the period of the structure (3.52 ± 0.01 μm), and its full-width-at-half-maximum (fwhm) was 30 nm, giving a quality factor ($Q = \lambda/\Delta\lambda$) of 118. As the sample was tilted, the peak split and the emissivity decreased rapidly. Since the bull's eye couples SPPs to only *p*-polarized light, the maximum emissivity of the structure should be ~0.5. As shown in Figure 2a, the emissivity of the peak for the normal angle (0.545) was slightly above this value, due to the background emissivity of W.

Calculated emission spectra for the same W bull's eye at various tilt angles were obtained via numerical simulation, using the experimental structural parameters listed in Figure 1b and the dielectric function of W for 900 °C.[31] We assumed that the bull's eye is much larger than the coherence length of the SPPs. This allowed effects due to the center and finite size of the structure to be neglected (see below). In this case, the bull's eye could be approximated as a series of linear gratings oriented around the center, and the absorptivity of these gratings averaged.[18] From this, the emissivity of the bull's eye could be estimated according to Kirchhoff's law.[6,7] As seen in Figure 2b, the calculated results were highly consistent with experiment. The calculated emission spectrum at $\theta = 0$ (normal) showed a single emission peak at 3.552 μm with a fwhm of 40 nm. When the sample was tilted, this emission peak split and decreased in emissivity, as observed in experiment.

The angular dependence of the emissivity at the peak wavelength is shown in Figure 2c. The measured and calculated spectra for normal emission showed a maximum emissivity of 0.545 at 3.532 μm and 0.547 at 3.552 μm, respectively. The fwhm angular divergence ($\Delta\theta$) of the emission peak for the measured and calculated emission spectra was estimated as 1.4 and 1.2°, corresponding to a SPP coherence length ($L_{SPP} = \lambda/\Delta\theta$) of 145 and 170 μm, respectively. The size of the bull's eye (2.1 mm) is much larger than these values, consistent with our assumption above. The difference in the measured and calculated coherence length is presumably due to structural imperfections and discrepancies between the experimental dielectric function and the literature values assumed (see also next paragraph).

Figure 2d shows the emission spectra of the bull's eye initially and after 12 h at 900 °C. After heating, the emission peak had a fwhm of 35 nm and shifted to 3.535 μm, indicating a peak broadening and red shift after thermal treatment. This change resulted from a deterioration of the W structure at elevated temperatures, as shown below. Figure 2d also includes the emission spectrum for a flat W film at 900 °C. Our flat W had larger emissivity than that calculated from the published dielectric function.[31] It is known that metallic films of the same element can exhibit different optical properties depending

DOI: 10.1021/acsphotonics.6b00022
ACS Photonics 2016, 3, 494−500

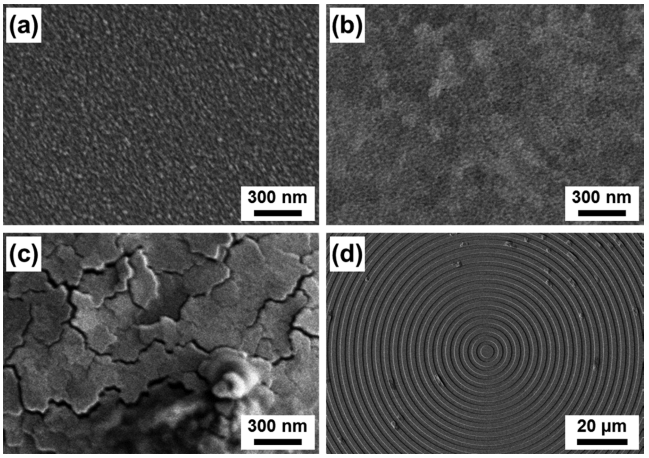

Figure 3. Scanning electron micrographs of a W bull's eye before and after heating. The surface of a ridge in the bull's eye (a) before and (b) after 12 h at 900 °C. (c) Magnified view of a cracked region and (d) a wider view of the bull's-eye pattern after 12 h at 900 °C. The bull's-eye pattern is maintained, but many cracked regions are observed.

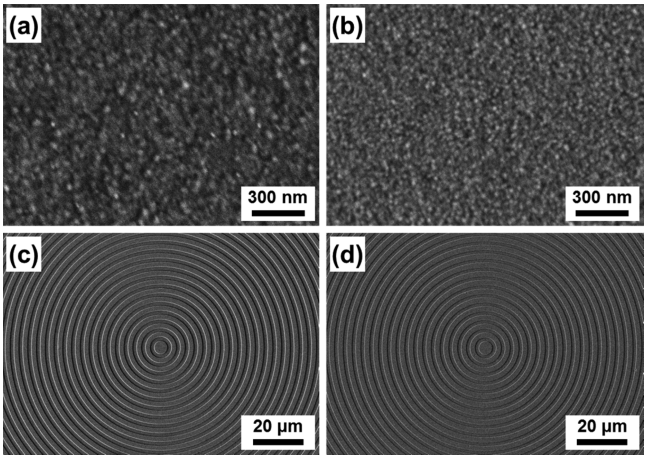

Figure 4. Scanning electron micrographs of HfO_2-coated W and Mo bull's eyes after 24 h at 900 °C, including magnified (a, b) and wider views (c, d) of the W and Mo structures, respectively. The HfO_2 thickness was 11 nm.

on the deposition conditions due to changes in porosity, surface roughness, grain boundaries, and so on.[29,30,32]

Figure 3a,b shows the surface morphology of a ridge in the W bull's eye before and after heating, respectively. The initial size of the grains was around 20 nm, consistent with our AFM data (Figure S1a in the Supporting Information). However, after heating at 900 °C for 12 h, the grains grew to ∼100 nm. This is detrimental because it can result in surface roughening and structure deformation. Another issue is the difference in thermal expansion between the W layer and the underlying silicon substrate. Indeed, stress at high temperatures caused cracks at some locations of the W bull's eye (Figure 3c,d).

Moreover, if the temperature is high enough, even small amounts of oxygen in the heating chamber can oxidize the metal surfaces, leading to deterioration of the thermal emission. Such oxidation was observed, especially for Mo bull's eyes. Even at 600 °C, the surface morphology changed significantly (Figure S3 in the Supporting Information) and the sample turned yellow, indicating oxidation.[33,34] This occurred not only at the surfaces but throughout the film due to the volatility of molybdenum oxide at high temperatures.[33] Thus, SPPs could no longer be excited after oxidization, prohibiting plasmonic thermal emission.

The thermal stability of high-temperature photonic structures, particularly photonic crystals, has been heavily studied.[25,35−41] Enhanced stability has been demonstrated by metal alloying or by adding a thin protective coating. To improve the stability of our bull's eyes, we followed the latter approach, introducing an oxide layer on the metal surface. Due to its high thermal stability, hafnium oxide (HfO_2) was chosen. Atomic layer deposition (ALD) was utilized, which can provide a uniform and continuous HfO_2 layer with an accurately controlled thickness.[42,43] An 11 nm thick HfO_2 layer was deposited on the metal surface, and the thermal stability of the bull's eye was then re-examined. Figure 4 shows the HfO_2-coated bull's eyes after heating. Even after 24 h at 900 °C, the W and Mo structures (including their grain sizes) has hardly changed (Figure 4a,b). This indicates that the HfO_2 layer, in addition to preventing oxidation, can suppress grain growth. Because small grains (with their many grain boundaries) can presumably better accommodate thermal stresses, grain growth can lead to cracks. HfO_2 is also a hard material, which can help suppress the expansion of the metallic layer. As a result, the HfO_2-coated bull's eyes can maintain their morphology at high temperatures for extended periods (Figure 4c,d).

Figure 5 presents emission spectra for the HfO_2-coated W bull's eye at 900 °C. The spectra versus tilt angle (Figure 5a) exhibited similar behavior to those of the bare W structure (Figure 2a). However, with the HfO_2 coating, the peak was broader (fwhm of 58 nm and Q of 61). This broadening is expected due to the decreased propagation length of SPPs on W with a high-dielectric layer such as HfO_2.[1] This also leads to an increase in the angular divergence (fwhm of 2.1°) and a decrease in the SPP coherence length to 97 μm (Figure 5c). These changes were also observed in the calculated emission spectra (Figure 5b,c); the calculated emission peak broadened (fwhm of 57 nm) and its angular divergence increased (1.5°). However, the introduction of the HfO_2 layer greatly improved the thermal stability of the structures. Even after 12 h at 900 °C (Figure 5d), the HfO_2-coated W bull's eye exhibited the same emission spectrum with no peak shift.

The HfO_2 coating also enhanced the thermal stability of our Mo structures. While a bare Mo bull's eye could not support SPPs even at 600 °C due to oxidation, the HfO_2 coating allowed tailored plasmonic thermal emission at 900 °C (Figure 6a). Compared to the HfO_2-coated W structure, the HfO_2-coated Mo bull's eye showed a slightly narrower emission peak (fwhm of 55 nm and Q of 65). In addition, the angular divergence was smaller (1.4°), giving an SPP coherence length of 145 μm (Figure 6c). The thermal stability of the HfO_2-coated Mo bull's eye was confirmed by heating at 900 °C for 12 h (Figure 6d). Based on these results, the HfO_2-coated Mo bull's eye can also provide an interesting infrared source.

Because the dielectric function of Mo at high temperatures is not available, we utilized the room-temperature values[27] and simulated the expected emission spectra (Figure 6b). Behavior similar to that observed in experiment was obtained, but the calculated results showed a narrower peak and smaller emissivity. SPP losses should increase with temperature, which is consistent with the broadening observed in experiment.

In general, these results show that bull's eyes can produce a directional narrowband source of thermal emission. However,

DOI: 10.1021/acsphotonics.6b00022
ACS Photonics 2016, 3, 494−500

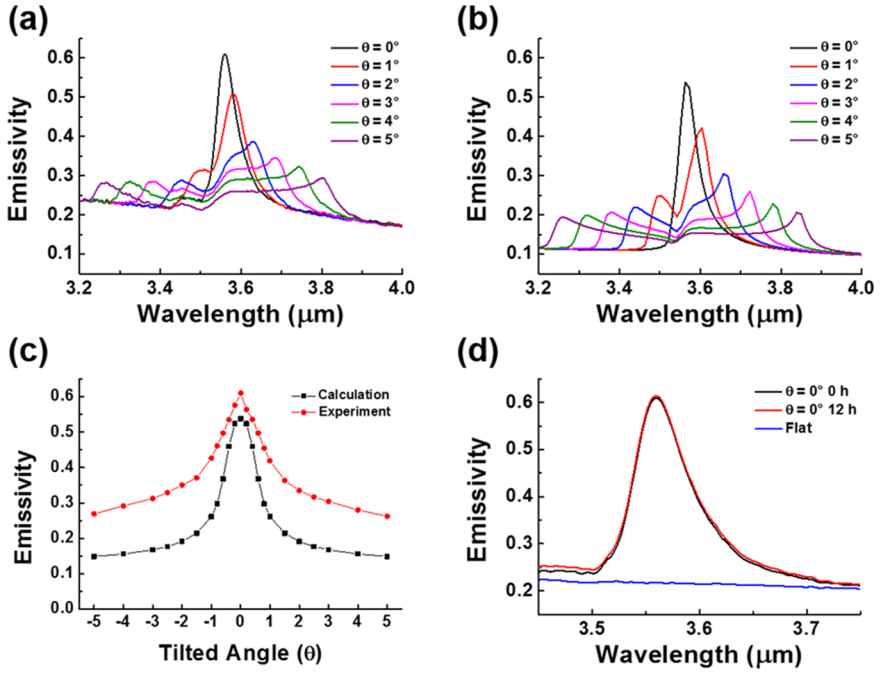

Figure 5. Thermal-emission spectra of a HfO_2-coated W bull's eye at 900 °C. The structure had a fill factor of 0.52, a groove depth of 180 nm, a period of 3.52 μm, and an 11 nm HfO_2 coating. (a) Measured thermal-emission spectrum at various tilt angles (θ) from normal, collected as in Figure 2a. (b) Calculated thermal-emission spectra vs θ. The dielectric function of W at 900 °C was employed and the dielectric constant of HfO_2 was approximated as 4 without an imaginary component. (c) Angular dependence of the emissivity at the peak wavelength. The measured and calculated spectra at $\theta = 0$ show a maximum emissivity of 0.610 at 3.559 μm and 0.538 at 3.563 μm, respectively. (d) Comparison of the emission spectra initially and after 12 h at 900 °C. The measured emission spectrum for a flat W film covered with the HfO_2 layer at 900 °C is also shown.

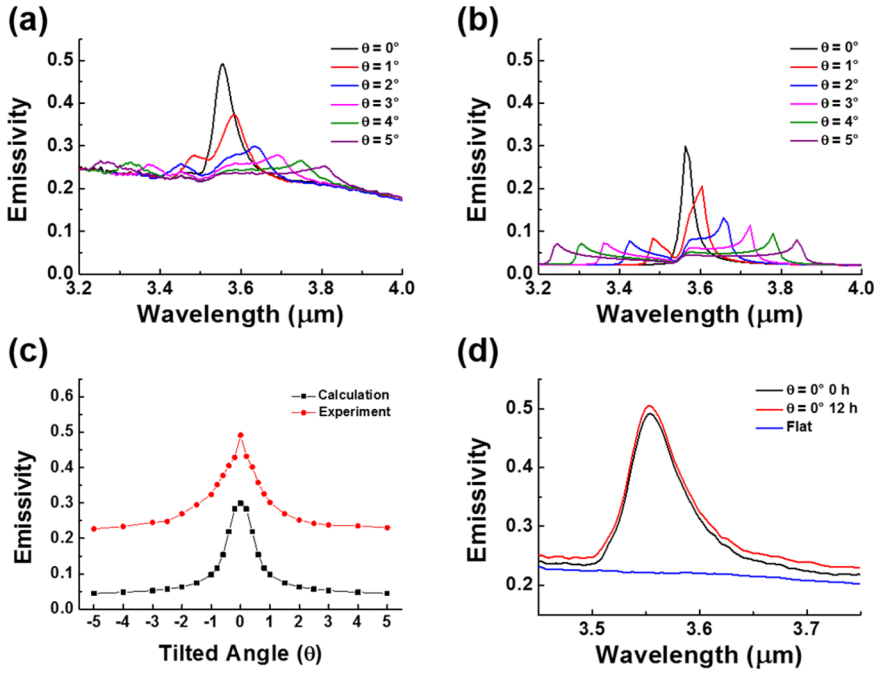

Figure 6. Thermal-emission spectra of a HfO_2-coated Mo bull's eye at 900 °C. The structure had a fill factor of 0.54, a groove depth of 180 nm, a period of 3.52 μm, and an 11 nm HfO_2 coating. (a) Measured thermal-emission spectra at various tilt angles (θ) from normal, collected as in Figure 2a. (b) Calculated thermal-emission spectra vs θ. The dielectric function of Mo at room temperature is employed and the dielectric constant of HfO_2 is approximated as 4 without an imaginary component. (c) Angular dependence of the emissivity at the peak wavelength. The measured and calculated spectra at $\theta = 0$ show a maximum emissivity of 0.492 at 3.554 μm and 0.299 at 3.563 μm, respectively. (d) Comparison of the emission spectra initially and after 12 h at 900 °C. The measured emission spectrum for a flat Mo film covered with the HfO_2 layer at 900 °C is also shown.

we note that due to the finite emissivity (~0.2) of W and Mo in the infrared, these devices also emit weakly in other directions and wavelengths. This effect is slightly worse for films with the HfO_2 coating. Thus, their efficiency (in terms of the amount of desired emission vs the total emission) is low. This could perhaps be improved by reflecting non-normal output to reheat

DOI: 10.1021/acsphotonics.6b00022
ACS Photonics 2016, 3, 494−500

the device. Alternatively, the effect could benefit from use of another plasmonic material with lower emissivity. Metals such as Ag or Au would provide this property. Unfortunately, they do not exhibit a sufficiently high melting point. Thus, W and Mo were chosen as the best compromise (for the same reasons they are used in incandescent light bulbs). We also note that in spectroscopic applications one often uses incandescent sources (e.g., quartz-tungsten-halogen bulbs) by filtering their output with a monochromator to select wavelength and direction. The efficiency of this process is also extremely low. One benefit of the bull's eye structure is that a narrowband source can be produced without a monochromator. Nevertheless, enhancing the efficiency of the bull's eye is an ongoing research goal.

CONCLUSION

We have demonstrated that bull's-eye thermal emitters can generate a highly directional narrowband beam of infrared light. This thermal beaming can be achieved simply by heating the bull's eye to excite SPPs. Due to the circular symmetry of the structure, the beam is emitted in the normal direction with a small angular divergence. The experimental results for W and Mo bull's eyes are highly consistent with theoretical predictions. Furthermore, a HfO_2 layer on the metal surfaces successfully prevents the deformation and oxidation of the metal structures, resulting in enhanced thermal stability. While here we have targeted 3.5 μm emission, the bull's eye is tunable with the periodicity of its grooves. The effect only requires that the metal is plasmonic at the desired wavelength and stable at the operational temperature. Because these devices are thin metallic films with low thermal mass, this temperature can be achieved by local resistive heating or by placing the structure in a hot environment. Consequently, such bull's eyes can provide novel incandescent light sources for various applications.

ASSOCIATED CONTENT

Supporting Information

The Supporting Information is available free of charge on the ACS Publications website at DOI: 10.1021/acsphotonics.6b00022.

Further details related to the fabrication, characterization, measurement, and simulation of our structures (PDF).

AUTHOR INFORMATION

Corresponding Author

*E-mail: dnorris@ethz.ch.

Notes

The authors declare no competing financial interest.

ACKNOWLEDGMENTS

The project was supported by the seventh Framework Programme of the European Commission under the HRC Power project. Preliminary data was obtained with support from the U.S. Department of Energy, Office of Basic Energy Sciences, Division of Materials Sciences and Engineering under Award DE-FG02-06ER46438. J.H.P. acknowledges the R&D Convergence Program of the National Research Council of Science and Technology of the Republic of Korea and a Korea Institute of Science and Technology internal project.

REFERENCES

(1) Raether, H. *Surface Plasmons*; Springer-Verlag: Berlin, 1988.

(2) Barnes, W. L.; Dereux, A.; Ebbesen, T. W. Surface plasmon subwavelength optics. *Nature* **2003**, *424*, 824−830.

(3) Novotny, L.; van Hulst, N. Antennas for light. *Nat. Photonics* **2011**, *5*, 83−90.

(4) Gramotnev, D. K.; Bozhevolnyi, S. I. Nanofocusing of electromagnetic radiation. *Nat. Photonics* **2013**, *8*, 13−22.

(5) Schuller, J. A.; Barnard, E. S.; Cai, W. S.; Jun, Y. C.; White, J. S.; Brongersma, M. L. Plasmonics for extreme light concentration and manipulation. *Nat. Mater.* **2010**, *9*, 193−204.

(6) Greffet, J. J.; Nieto-Vesperinas, M. Field theory for generalized bidirectional reflectivity: derivation of Helmholtz's reciprocity principle and Kirchhoff's law. *J. Opt. Soc. Am. A* **1998**, *15*, 2735−2744.

(7) Han, S. E. Theory of thermal emission from periodic structures. *Phys. Rev. B: Condens. Matter Mater. Phys.* **2009**, *80*, 155108.

(8) Kreiter, M.; Oster, J.; Sambles, R.; Herminghaus, S.; Mittler-Neher, S.; Knoll, W. Thermally induced emission of light from a metallic diffraction grating, mediated by surface plasmons. *Opt. Commun.* **1999**, *168*, 117−122.

(9) Heinzel, A.; Boerner, V.; Gombert, A.; Blasi, B.; Wittwer, V.; Luther, J. Radiation filters and emitters for the NIR based on periodically structured metal surfaces. *J. Mod. Opt.* **2000**, *47*, 2399−2419.

(10) Laroche, M.; Arnold, C.; Marquier, F.; Carminati, R.; Greffet, J. J.; Collin, S.; Bardou, N.; Pelouard, J. L. Highly directional radiation generated by a tungsten thermal source. *Opt. Lett.* **2005**, *30*, 2623−2625.

(11) Liu, X. L.; Tyler, T.; Starr, T.; Starr, A. F.; Jokerst, N. M.; Padilla, W. J. Taming the blackbody with infrared metamaterials as selective thermal emitters. *Phys. Rev. Lett.* **2011**, *107*, 045901.

(12) Greffet, J. J.; Carminati, R.; Joulain, K.; Mulet, J. P.; Mainguy, S. P.; Chen, Y. Coherent emission of light by thermal sources. *Nature* **2002**, *416*, 61−64.

(13) Dahan, N.; Niv, A.; Biener, G.; Kleiner, V.; Hasman, E. Space-variant polarization manipulation of a thermal emission by a SiO_2 subwavelength grating supporting surface phonon-polaritons. *Appl. Phys. Lett.* **2005**, *86*, 191102.

(14) Rephaeli, E.; Fan, S. H. Absorber and emitter for solar thermophotovoltaic systems to achieve efficiency exceeding the Shockley-Queisser limit. *Opt. Express* **2009**, *17*, 15145−15159.

(15) Granier, C. H.; Afzal, F. O.; Min, C. J.; Dowling, J. P.; Veronis, G. Optimized aperiodic highly directional narrowband infrared emitters. *J. Opt. Soc. Am. B* **2014**, *31*, 1316−1321.

(16) Costantini, D.; Lefebvre, A.; Coutrot, A. L.; Moldovan-Doyen, I.; Hugonin, J. P.; Boutami, S.; Marquier, F.; Benisty, H.; Greffet, J. J. Plasmonic metasurface for directional and frequency-selective thermal emission. *Phys. Rev. Appl.* **2015**, *4*, 014023.

(17) Streyer, W.; Feng, K.; Zhong, Y.; Hoffman, A. J.; Wasserman, D. Selective absorbers and thermal emitters for far-infrared wavelengths. *Appl. Phys. Lett.* **2015**, *107*, 081105.

(18) Han, S. E.; Norris, D. J. Beaming thermal emission from hot metallic bull's eyes. *Opt. Express* **2010**, *18*, 4829−4837.

(19) Lezec, H. J.; Degiron, A.; Devaux, E.; Linke, R. A.; Martin-Moreno, L.; Garcia-Vidal, F. J.; Ebbesen, T. W. Beaming light from a subwavelength aperture. *Science* **2002**, *297*, 820−822.

(20) Martin-Moreno, L.; García-Vidal, F. J.; Lezec, H. J.; Degiron, A.; Ebbesen, T. W. Theory of highly directional emission from a single subwavelength aperture surrounded by surface corrugations. *Phys. Rev. Lett.* **2003**, *90*, 167401.

(21) Chang, Y. T.; Ye, Y. H.; Tzuang, D. C.; Wu, Y. T.; Yang, C. H.; Chan, C. F.; Jiang, Y. W.; Lee, S. C. Localized surface plasmons in Al/Si structure and $Ag/SiO_2/Ag$ emitter with different concentric metal rings. *Appl. Phys. Lett.* **2008**, *92*, 233109.

(22) Aouani, H.; Mahboub, O.; Bonod, N.; Devaux, E.; Popov, E.; Rigneault, H.; Ebbesen, T. W.; Wenger, J. Bright unidirectional fluorescence emission of molecules in a nanoaperture with plasmonic corrugations. *Nano Lett.* **2011**, *11*, 637−644.

(23) Harats, M. G.; Livneh, N.; Zaiats, G.; Yochelis, S.; Paltiel, Y.; Lifshitz, E.; Rapaport, R. Full spectral and angular characterization of

DOI: 10.1021/acsphotonics.6b00022
ACS Photonics 2016, 3, 494−500

highly directional emission from nanocrystal quantum dots positioned on circular plasmonic lenses. *Nano Lett.* **2014**, *14*, 5766−5771.
(24) Yi, J. M.; Cuche, A.; Devaux, E.; Genet, C.; Ebbesen, T. W. Beaming visible light with a plasmonic aperture antenna. *ACS Photonics* **2014**, *1*, 365−370.
(25) Denny, N. R.; Han, S. E.; Norris, D. J.; Stein, A. Effects of thermal processes on the structure of monolithic tungsten and tungsten alloy photonic crystals. *Chem. Mater.* **2007**, *19*, 4563−4569.
(26) Maier, S. A. *Plasmonics: Fundamentals and Applications*; Springer Science: New York, 2007.
(27) Palik, E. D. *Handbook of Optical Constants of Solids*; Academic Press: Orlando, FL, 1985.
(28) Nagpal, P.; Lindquist, N. C.; Oh, S.-H.; Norris, D. J. Ultrasmooth patterned metals for plasmonics and metamaterials. *Science* **2009**, *325*, 594−597.
(29) Park, J. H.; Nagpal, P.; Oh, S.-H.; Norris, D. J. Improved dielectric functions in metallic films obtained via template stripping. *Appl. Phys. Lett.* **2012**, *100*, 081105.
(30) Park, J. H.; Nagpal, P.; McPeak, K. M.; Lindquist, N. C.; Oh, S.-H.; Norris, D. J. Fabrication of smooth patterned structures of refractory metals, semiconductors, and oxides via template stripping. *ACS Appl. Mater. Interfaces* **2013**, *5*, 9701−9708.
(31) Aksyutov, L. N. Temperature dependence of the optical constants of tungsten and gold. *J. Appl. Spectrosc.* **1977**, *26*, 656−660.
(32) McPeak, K. M.; Jayanti, S. V.; Kress, S. J. P.; Meyer, S.; Iotti, S.; Rossinelli, A.; Norris, D. J. Plasmonic films can easily be better: Rules and recipes. *ACS Photonics* **2015**, *2*, 326−333.
(33) Gulbransen, E. A.; Andrew, K. F.; Brassart, F. A. Oxidation of molybdenum 550 to 1700 °C. *J. Electrochem. Soc.* **1963**, *110*, 952−959.
(34) Heyns, J. B. B.; Cruywagen, J. J. Yellow molybdenum(VI) oxide dihydrate. In *Inorganic Syntheses*; Shreeve, J. M., Ed.; John Wiley & Sons: Hoboken, NJ, 1986; Vol. *24*, pp 191−192.
(35) Denny, N. R.; Li, F.; Norris, D. J.; Stein, A. In situ high temperature TEM analysis of sintering in nanostructured tungsten and tungsten-molybdenum alloy photonic crystals. *J. Mater. Chem.* **2010**, *20*, 1538−1545.
(36) Nagpal, P.; Josephson, D. P.; Denny, N. R.; DeWilde, J.; Norris, D. J.; Stein, A. Fabrication of carbon/refractory metal nanocomposites as thermally stable metallic photonic crystals. *J. Mater. Chem.* **2011**, *21*, 10836−10843.
(37) Arpin, K. A.; Losego, M. D.; Braun, P. V. Electrodeposited 3D tungsten photonic crystals with enhanced thermal stability. *Chem. Mater.* **2011**, *23*, 4783−4788.
(38) Rinnerbauer, V.; Yeng, Y. X.; Chan, W. R.; Senkevich, J. J.; Joannopoulos, J. D.; Soljacic, M.; Celanovic, I. High-temperature stability and selective thermal emission of polycrystalline tantalum photonic crystals. *Opt. Express* **2013**, *21*, 11482−11491.
(39) Arpin, K. A.; Losego, M. D.; Cloud, A. N.; Ning, H. L.; Mallek, J.; Sergeant, N. P.; Zhu, L. X.; Yu, Z. F.; Kalanyan, B.; Parsons, G. N.; Girolami, G. S.; Abelson, J. R.; Fan, S. H.; Braun, P. V. Three-dimensional self-assembled photonic crystals with high temperature stability for thermal emission modification. *Nat. Commun.* **2013**, *4*, 2630.
(40) Stelmakh, V.; Rinnerbauer, V.; Geil, R. D.; Aimone, P. R.; Senkevich, J. J.; Joannopoulos, J. D.; Soljacic, M.; Celanovic, I. High-temperature tantalum tungsten alloy photonic crystals: Stability, optical properties, and fabrication. *Appl. Phys. Lett.* **2013**, *103*, 123903.
(41) Garin, M.; Hernandez, D.; Trifonov, T.; Alcubilla, R. Three-dimensional metallo-dielectric selective thermal emitters with high-temperature stability for thermophotovoltaic applications. *Sol. Energy Mater. Sol. Cells* **2015**, *134*, 22−28.
(42) Hausmann, D. M.; Kim, E.; Becker, J.; Gordon, R. G. Atomic layer deposition of hafnium and zirconium oxides using metal amide precursors. *Chem. Mater.* **2002**, *14*, 4350−4358.
(43) Kukli, K.; Ritala, M.; Sajavaara, T.; Keinonen, J.; Leskela, M. Atomic layer deposition of hafnium dioxide films from hafnium tetrakis(ethylmethylamide) and water. *Chem. Vap. Deposition* **2002**, *8*, 199−204.

DOI: 10.1021/acsphotonics.6b00022
ACS Photonics 2016, 3, 494−500